Long axial imaging range using conventional swept source lasers in optical coherence tomography via re-circulation loops

Adrian Bradu*[a], David A. Jackson[a], and Adrian Podoleanu[a]
[a]Applied Optics Group, School of Physical Sciences, University of Kent, Canterbury, CT2 7NH United Kingdom
* Corresponding author's email address: a.bradu@kent.ac.uk

ABSTRACT

Typically, swept source optical coherence tomography (SS-OCT) imaging instruments are capable of a longer axial range than their camera based (CB) counterpart. However, there are still various applications that would take advantage for an extended axial range. In this paper, we propose an interferometer configuration that can be used to extend the axial range of the OCT instruments equipped with conventional swept-source lasers up to a few cm. In this configuration, the two arms of the interferometer are equipped with adjustable optical path length rings. The use of semiconductor optical amplifiers in the two rings allows for compensating optical losses hence, multiple paths depth reflectivity profiles (A-scans) can be combined axially. In this way, extremely long overall axial ranges are possible. The use of the re-circulation loops produces an effect equivalent to that of extending the coherence length of the swept source laser. Using this approach, the achievable axial imaging range in SS-OCT can reach values well beyond the limit imposed by the coherence length of the laser, to exceed in principle many centimeters. In the present work, we demonstrate axial ranges exceeding 4 cm using a commercial swept source laser and reaching 6 cm using an "in-house" swept source laser. When used in a conventional set-up alone, both these lasers can provide less than a few mm axial range.

Keywords: optical coherence tomography, re-circulation rings, long axial range, coherence length

1. INTRODUCTION

For some applications, the axial range that can be achieved by conventional spectral (Fourier) domain optical coherence tomography can prove insufficient. Long axial range imaging is necessary for example in endoscopy, small animal imaging, or anterior segment imaging of the human eye where sometimes axial ranges of over 1 cm, with acceptable sensitivity over the entire depth are required.

Unfortunately, there are limitations on obtaining infinitely long axial ranges, especially in camera based OCT instruments, where the limitation of the axial range is due to the finite spectral resolution of the spectrometer and (or) the pixel width of the line-scan camera. Longer axial ranges are possible in swept source OCT instruments, where the axial range is now determined by the instantaneous line-width of the swept source laser. A plethora of narrow line-width SSs were reported, which makes SS-OCT more suitable to imaging long axial samples rather than CB-OCT. However, in SS-OCT, by increasing the wavelength tuning speed, the coherence length associated with the instantaneous line-width decreases.

The strength of interference decays with the optical path difference (OPD) between the reference arm length and object arm length of the interferometer and this leads to a decay of the signal-to-noise ratio. New tunable vertical-cavity surface emitting lasers (VCSEL) and akinetic light sources, can provide axial ranges exceeding 1 cm [1-2]. However, both VCSELs and akinetic sources are more expensive than the conventional microelectromechanical systems (MEMS) based swept sources widely available.

Here, we present an interferometric configuration that allows simultaneous interrogation of multiple depths separated by an interval adjustable from zero to values less, larger or much larger than the coherence length of the swept source and increase of the axial imaging range beyond the limit imposed by the coherence length of the SS. A demonstration of obtaining extra-long axial ranges when using conventional commercial and "in-house" swept source lasers is presented. For this purpose, two interferometric configurations were devised and proposed for two spectral ranges:

A. Central wavelength 1050 nm (conventional commercial swept source employed)

B. Central wavelength 1550 nm (conventional "in-house" swept source employed)

In both cases, in theory, by using recirculation loops in both sample and reference arms of the interferometers, an infinitely long imaging axial range becomes achievable. We demonstrate that both instruments, although equipped with conventional swept source lasers, are capable of providing values of the axial range similar to those provided by systems driven by VCSEL and akinetic light sources.

2. METHODS

For this study, we devised two SS-OCT imaging instruments.

A. The first instrument uses a commercial Swept source laser (Broadsweep, Superlum, Cork, Ireland) with a central wavelength of 1060 nm, sweeping range 60 nm and instantaneous line-width 0.05 nm which determines an associated coherence length of around 20 mm.

B. The second configuration uses an "in-house" developed swept source laser. This swept source, has a central wavelength at 1550 nm, sweeping range 60 nm and instantaneous line-width 0.1 nm, which determines an associated coherence length of around 20 mm.

A common schematic diagram of the two instruments is depicted in Fig. 1. In both cases, light from the swept source is split into a main sample arm and a main reference arm by the directional coupler DC, which feeds a Mach-Zehnder interferometer set-up. In each arm of the interferometer, separate optical rings, with adjustable optical path length are placed. In each ring, an acousto-optic frequency shifter ($AOFS_1$ and $AOFS_2$) that shift the optical frequency upward by the frequency of the driving signal f_1 (f_2) are incorporated.

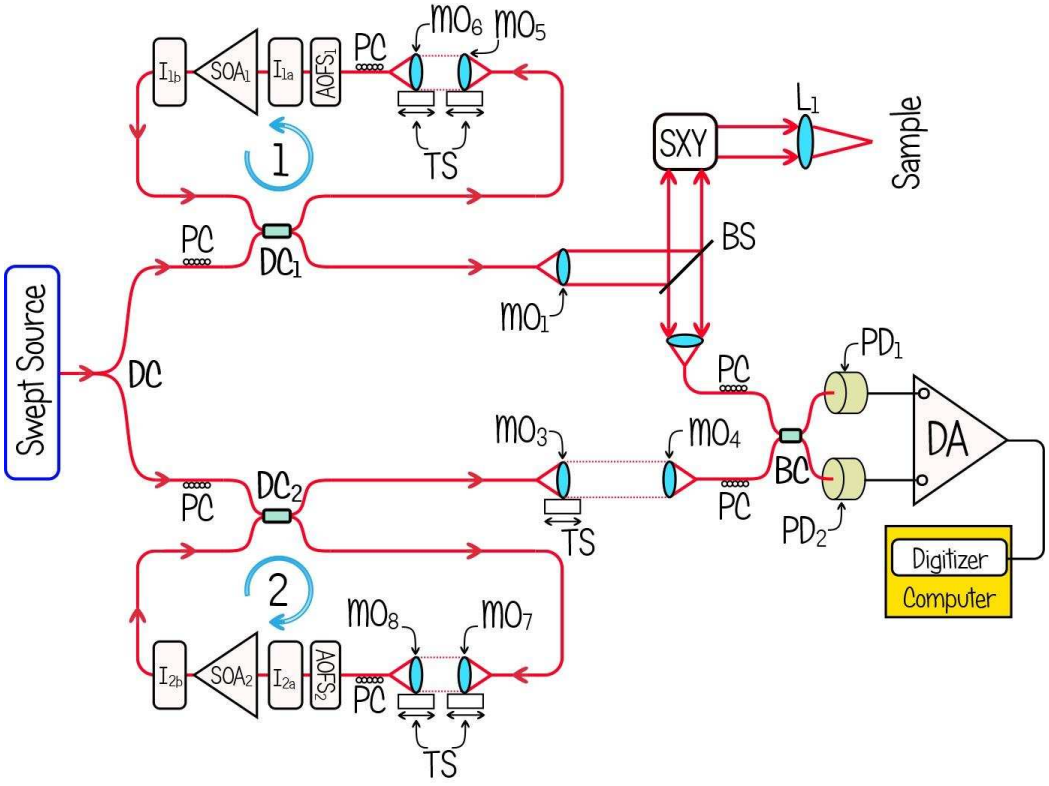

Figure 1. Schematic diagram of the SS-OCT instrument: DCs, BC: 50:50 couplers, PC: polarization controllers, $I_{1,2(a,b)}$: optical isolators, $SOA_{1,2}$: optical amplifiers, $AOFS_{1,2}$: frequency shifters, MO1-8: microscope objectives, TS: translation stages, L_1: lens, BS: beam-splitter, $PD_{1,2}$: photo-detectors, DA: differential amplifier, SXY: galvo-scanner. The choice of the optical isolators, semiconductor optical amplifiers, optical fiber and optical isolators is dictated by the configuration used (A or B).

To compensate for optical losses, semiconductor optical amplifiers are used.

A. For configuration A, two semiconductor amplifiers from QPhotonics (model QSOA-1050) are employed. The optical fiber used for this configuration is HI-1060.

B. For the second configuration, B, the optical losses in the rings are compensated by SOA_1 and SOA_2, BT model SOA-S-OEC-1550. The optical fiber used for this configuration is SMF-28.

The amplifiers have to compensate for the optical losses due to the imperfect light injection into the optical fibers via the microscope objectives MO_6 and MO_8 respectively, and for the losses due to the frequency shifters. They also have to compensate, for each recirculation for the light directed towards the main interferometer (the directional couplers DC_1 and DC_2 have a splitting ratio of 50%). The injection of light into the rings and the reinjection of the amplified light into the interferometer take place in the directional couplers DC_1 (DC_2). For every pass of the light through the two loops, the optical frequency is shifted by a quantity f_1 and respectively f_2.

By adjusting the optical path difference OPD_R between the two rings, it is possible to simultaneously interrogate multiple axial depths [3]. These depth profiles are separated exactly by the difference between the optical path lengths of the two rings, OPD_R.

In both configurations, the optical path lengths in the loops and their difference OPD_R can be tweaked by altering the position of the micrometer precision translation stages TS incorporated in the rings, which allow axial movement of the launchers holding the microscope objectives (MO_5-MO_8) and respective optical fiber apertures. The two optical isolators $I_{1a,b}$ ($I_{2a,b}$) placed in each ring, at the input and at the output of the SOA_1 (SOA_2) are employed to protect their operation from stray reflections and stop counter propagating waves into the rings.

In the sample arm of the interferometer, a beam-splitter (BS) is employed together with two microscope objectives (MO_1 and MO_2), a pair of orthogonal galvo-scanner mirrors (SXY) and an achromatic lens (L_1) to direct light to and back from the sample to be investigated. For both cases, the optical power on the sample was around 1 mW. The multiple waves from the reference path interfere with the multiple waves from the sample path at the directional coupler BC, producing a beat signal at a frequency $|f_1-f_2| = n\Delta f$, where n is the number of re-circulations of light in the two rings. The output signals from BC are conveyed to a balanced photo-detector unit, consisting of two photo-detectors (PD_1 and PD_2), and a differential amplifier (DA). The differential amplifier's output signal is digitized using a 12-bit analog-to-digital fast acquisition card (National Instruments, Austin, Texas, model PCI-5124). The digitizer was triggered for each channelled spectrum, synchronously with the trigger signal associated with the signal which drives the tunable filter of the swept sources. Multiple signals placed around carriers of frequency $n\Delta f$ are all present in the signal photo-detected by DA. Both systems are compensated for unbalanced dispersion. Each channeled spectrum is resampled to compensate for nonlinearities and Fast Fourier Transformed (FFT) are used to produce A-scans corresponding to the interference of signals from the main interferometer (light that is not re-circulated) as well as to the A-scans corresponding to the light re-circulated by the loops.

3. RESULTS AND DISCUSSION

Figure 2 depicts the FFT of the digitized photo-detected signal when a highly reflecting sample (flat mirror) is used as object, for an OPD = 0 in the main loop and $OPD_R = 0$ in the rings. For configuration A, the two AOFS were driven initially at $f_1 = 40$ MHz and $f_2 = 40.5$ MHz respectively, while for configuration B, at $f_1 = 40$ MHz and $f_2 = 40.275$ MHz respectively. The component around 0 Hz (order n = 0) corresponds to the interference of waves originating from the main loop only (not re-circulated light) while the other peaks at multiples of $\Delta f = 500$ kHz (orders 1 ... 5) for configuration A and $\Delta f = 275$ kHz (orders n = 1 … 36) for configuration B are generated by interference of similar orders, n, of re-circulation waves in the rings. In both configurations, depending on the balance of gain and losses in the rings, a limited number of round trips can be achieved. For the instrument devised at 1550 nm (configuration B), an attenuation of only 0.5 – 1 dB (Fig. 2B) is noticed from one recirculation to the next. This is a large improvement over the attenuation observed on configuration A, at 1050 nm where an attenuation of 6 - 8 dB is noticed (Fig. 2A).

By increasing the OPD in the main loop, all frequency components in Figs. 2A and 2B move to the right by the same frequency, $F = C \cdot OPD$ as determined by a factor C, where C is the conversion factor from OPD to RF due to scanning the number of peaks in the channeled spectrum determined by the given OPD. As there are no acousto-optics frequency shifters in the main loop, the interference of the two beams in the main loop exhibits mirror terms, and therefore, irrespective of the OPD sign, the peak of initial frequency zero will move to the right. However, on all other (secondary)

peaks, the detected signal is free of mirror terms. By adjusting the optical path difference OPD_R, between the two rings, in both configurations, the combined fundamental/high order channel signal can be generated.

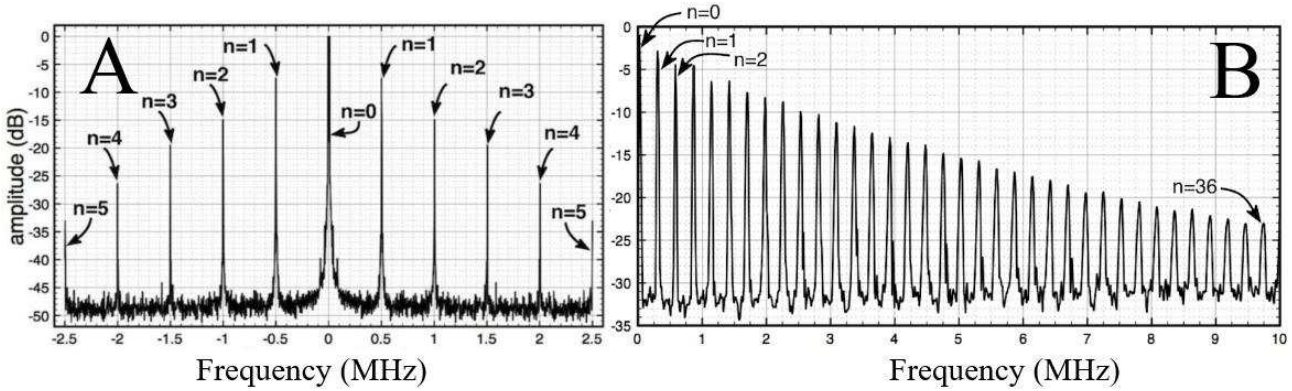

Figure 2. FFT of the photo-detected signal for OPD_R = OPD = 0.

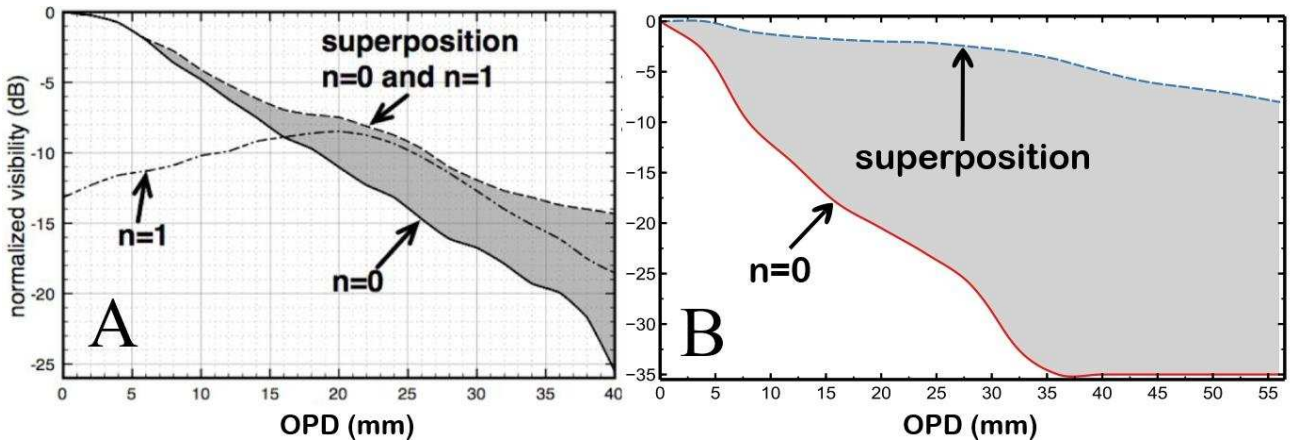

Figure 3. Sensitivity drop-off vs OPD for the fundamental mode (top) and combined situation (bottom)

The most interesting configuration providing the longest axial range is obviously B. In this case, by adjusting the OPD_R between the two loops, to -8.8 mm, the interference for the re-circulating waves traversing the rings once exhibit a maximum amplitude at OPD = 8.8 mm, the re-circulating waves traversing the rings twice will exhibit an interference maximum at OPD = 17.6 mm, and so on. Thus, by maintaining OPDR = - 8.8 mm, profiles of sensitivity of A-scans demodulated around various carrier frequencies $n\Delta f$ (n = 0, 1, 2…) can be generated.

In Fig. 3 the sensitivity drop-off vs OPD while no recirculation loops are used is presented for the two configurations (configuration A in Fig. 3A and configuration B in Fig. 3B). In configuration A, sensitivity decays by 6 dB for an OPD of around 12 mm. By engaging the re-circulation loops, for the same OPD, a small improvement in sensitivity of around 1 dB is observed. At longer values of the OPD, such as around 40 mm, without re-circulating the light, a fall in sensitivity of around 25 dB compared to OPD=0 is noticed. By engaging the re-circulation loops, a gain in sensitivity of 12 dB is obtained (Fig. 3A).

The improvement in sensitivity is more noticeable for the second configuration presented here, B. For this case, the sensitivity decreases slower, by 6 dB for an OPD of around 6-7 mm. When the recirculation loops are engaged (the fundamental and the high order channels are engaged), only after 60 mm the sensitivity drops by 6 dB. This can be seen as a x10 enlargement of the axial range.

4. CONCLUSION

Both configurations ensure a very long axial range when the re-circulation loops are engaged (making use of both the fundamental and the higher order channels). Configuration B, using an “in-house” swept laser with its central wavelength at 1550 nm provides a longer axial range (sensitivity drops by 6 dB at OPD = 50 mm). The other

configuration presented here (A), ensures a drop of the sensitivity by 6 dB at OPD = 15 mm. In both cases, the axial range is extended well beyond the limit imposed by the coherence length of the swept source which in our study was around 20 mm. Both configurations have the potential to deliver distinct images for different axial range.

Although configuration B shows better enhancement in sensitivity than configuration A, further research is required to enhance the number of roundtrips and their corresponding amplitudes for configurations where shorter wavelengths (eventually in the 800 nm range) are employed.

The limitation in the number of peaks at shorter wavelengths is due to the limited gain and the large amount of spontaneous emitted light of the semiconductor optical amplifiers used in the present study. By using better optical amplifiers, lower cost swept sources, with relatively wide line-width, determining small axial range values, even sub-millimeter, could be enhanced by using the proposed re-circulation based method presented here. In this way, imaging over a few millimeters, axial range typical for the current OCT applications, with sufficient sensitivity will be possible. The proposed configuration can be used to enhance the axial range of the existent OCT imaging instruments. The current commercial swept sources are already able to provide a few mm axial resolution. The method we propose here can be used to make them usable for applications requiring longer, centimeters depth range.

ACKNOLEDGEMENTS

The authors thank the EPSRC Grants (REBOT) EP/N019318/1 and EP/N019229/1. AP acknowledges the UBAPHODESA Marie Curie, European Industrial Doctorate 607627, the ERC Proof-of-Concept`AdaSmartRes' 754695. AP is also supported by the NIHR Biomedical Research Centre (BRC) at Moorfields Eye Hospital NHS Foundation Trust, UCL Institute of Ophthalmology and the Royal Society Wolfson Research Merit Award.

REFERENCES

[1] Ahsen, O.O., Tao, Y.K., Potsaid, B.M., Sheikine, Y., Jiang, J., Grulkowski, I., Tsai, T.-H., Jayaraman, V., Kraus, M.F., Connolly, J.L., Hornegger, J., Cable, A. and Fujimoto, J.G., "Swept source OCM using a 1310 nm VCSEL light source," Opt. Express 21(15), 18021–18033 (2013).

[2] Bonesi, M., Minneman, M.P., Ensher, J., Zabihian, B., Sattmann, H., Boschert, P., Hoover, E., Leitgeb, R.A., Crawford, M. and Drexler, W., "Akinetic all-semiconductor programmable swept-source at 1550 nm and 1310 nm with centimeters coherence length," Opt. Express 22(3), 2632–2655 (2014).

[3] Bradu, A., Neagu, L. and Podoleanu, A., "Extra-long imaging range swept source optical coherence tomography using re-circulation loops," Opt. Express 18, 25361-25370 (2010).